Paper ID: FM-13

Experimental Studies on Heat Transfer and Friction Factor in a Turbulent Flow Through a Smooth Square Duct

A.K.M. Abdul Hamid[1], M.A. Taher Ali[2], A. R. Akanda[3] and M. Riaz Pervez[4]
[1, 4] Department of Mechanical Engineering, RUET, Rajshahi-6204, Bangladesh
[1]E-mail: mahamid_ruet@yahoo.com
[4]E-mail: mrp@ruet.ac.bd
[2] Department of Mechanical Engineering, BUET, Dhaka -1000,
Road N0.3, House N0.21/A, Dhanmondi, Dhaka, Bangladesh.
E-mail: matali@me.buet.ac.bd
[3] Sonargaon University, 71 Kawranbazer, Tejgaon, Dhaka-1215
Email: akhanda@iut-dhaka.edu

Abstract

The forced convective heat transfer is studied experimentally and the measurements are presented of the distributions of local as well as average heat transfer coefficients and the friction factors for a fully developed turbulent flow in an asymmetrically heated smooth square duct at constant heat flux as a boundary condition. In the present experimental investigation it is found that on average, with 57 percent increase in Reynolds Number the static pressure drop is increased by 186 percent and the Nusselt's number is increased by 41 percent. In the present investigation the friction factor obtained increases with the increase of Reynolds Number instead of published data where it decreases or approaches a constant value for smooth noncircular ducts. The results are presented in their final concise form of compact correlations that involve dimensionless groups which represent the characteristics of heat transfer and friction factors. The correlations can be used for improved numerical analysis and for better design of heat transfer equipment's for engineering applications.

Keywords: Force Convective Heat Transfer, Friction Factor, Turbulent Flow, Smooth Square duct.

1. Introduction

In the fluid mechanics and heat transfer several variables are combined into a few dimensionless parameters and the results are presented in the form of empirical equations that involve both individual variable parameters and dimensionless groups. No doubt this technique considerably reduces the number of variables involved in the experimental investigations but does not demonstrate how the characteristics of individual flow parameter behaves with respect to each other in complex situations with imposed boundary conditions. Thus an attempt has been made to study experimentally some of the most important flow parameters such as Nusselt's number, friction factor, Stanton number etc, for a turbulent flow through a smooth square duct. The gathered data will be useful for those pursuing the task of numerical prediction in this area of research and development. The object is to provide a good understanding on the characteristics of some of these variable flow parameters as well as on how they are related to each other when the duct is heated asymmetrically under constant heat flux boundary conditions.

2. Literature Survey

The turbulent flow as well as the temperature field in non-circular ducts is influenced by the existence of the secondary flow [3]. Though the velocity of this secondary flow is a small percentage of the primary flow velocity, of the order of 2 to 3 percent, its influence on the flow and temperature fields in the duct cannot be ignored [9]. This is the reason why these variable flow parameters have attracted interest not only for the light they shed on fluid dynamics, but also in relation to the augmentation of heat transfer [6]. Although, in ducts, secondary flow would affect the characteristics of the forced convective heat transfer, as has already been found by many investigators, there are only a few reports on fundamental ducts [7]. It has been recently found that in exactly the same experimental set up and configuration with constant heat flux boundary condition the Prandtl number does not remain constant [2] but it rather decreases with increase of Reynolds Number as well as with increase of location of positions y/B from center towards the side walls. In view of the above discussion, a need therefore exist for an experimental investigation to incorporate Prandtl number as an important variable parameter to obtain improve correlations for correct analysis of heat transfer problems in engineering applications.

3. Experimental Set Up and Methodology

The experimental set up has been designed and instruments and probes are installed in it and these are connected with a high speed digital computer. A schematic diagram of the straight experimental setup of length $9735\ mm$ is illustrated in the Fig: 1. Hydro-dynamically fully developed velocity profiles are attained at about $2500\ mm$ downstream from the duct entrance. Thus the test section of the duct of length 4869 mm having inner cross section area of $50\ mm \times 50\ mm$ consists of heated portion of length $1833\ mm$ and unheated portion of $3036\ mm$. The unheated portion of the duct serves to establish hydro-dynamically fully developed flow at the entrance to the heated section. At the working section, at x=1725 mm downstream from the leading edge of the heated portion of the test section, the flow is assumed to be fully developed both hydro-dynamically and thermally. Fig: 2 illustrates the details of the cross sectional view of the heated test section. The heating effect is symmetrical about z-axis but non-symmetric about x- and y- axes,

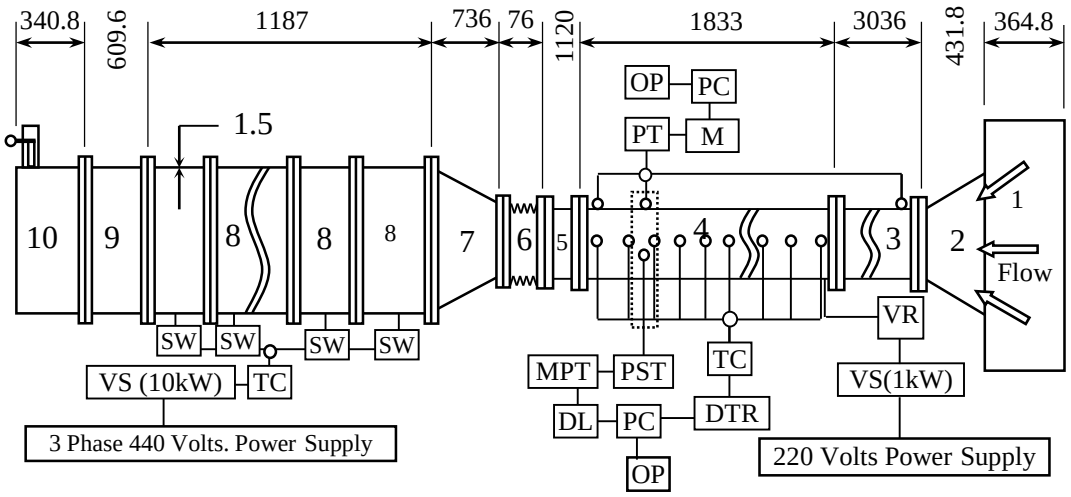

Legend — All Dimension are in mm

1. Air Filter	8. Fans 9. Silencer	DL = Data Logger
2. Inlet Contractor	10. Butter Fly	PC = Personal Computer
3. Unheated Duct	TC = Thermo-couple	OP = Out-put
4. Heated Test Duct	DTR = Digital Temperature Recorder	PT = Pitot Tube
5. Unheated Duct	PST = Pilot Static Tube	SW = Switch
6. Bellow	MPT = Micro Pressure Transducer	VS = Voltage Stabilizer
7. Diffuser	M = Manometer	VR = Voltage Regulator

Fig: 1 Schematic Diagram of the Experimental Setup

Fig:3. to maintain a constant heat flux a voltage stabilizer followed by a voltage regulator, both having 1kW capacity is used for constant power supply to the heater. The flat nichrome wire of size 28 SWG having the resistance of 9.8097 Ω/m is used to achieve uniform wall temperature condition.

As the thermocouple is attached intrinsically with the pitot static tube, the measurements of both the velocity and the temperature of the air flowing through the duct are taken simultaneously. Thermocouples are used to measure both wall and air temperature. Two pressure tapings one at the entry and the other at x=4761mm downstream from the leading edge of the test section are used for the static pressure drop measurement.

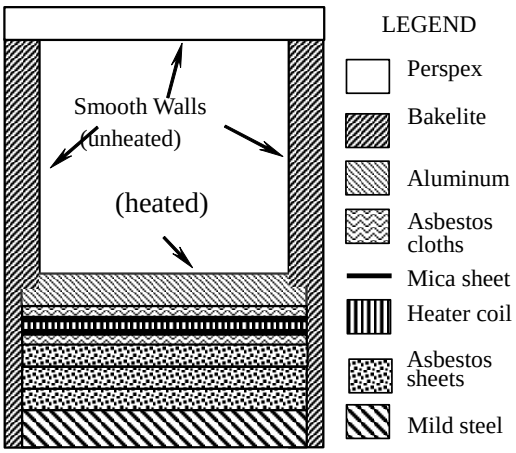

Fig: 2 Illustrating the Cross sectional View of Duct

The heating effect is symmetrical about z-axis but non-symmetric about x- and y- axes, Fig: 3. the presence of the bottom heated wall creates asymmetric flow field. To maintain a constant heat flux a voltage stabilizer followed by a voltage regulator, both having 1kW capacity is used for constant power supply to the heater. The flat nichrome wire of size 28 SWG having the resistance of 9.8097 Ω/m is used to achieve uniform wall temperature condition. As the thermocouple is attached intrinsically with the pitot static tube, the measurements of both the velocity and the temperature of the air flowing through the duct are taken simultaneously. Thermocouples are

used to measure both wall and air temperature. Two pressure tapings one at the entry and the other at the working section i.e., x=4761mm downstream from the leading edge of the test section are used for the static pressure drop measurement.

4. Measurement System

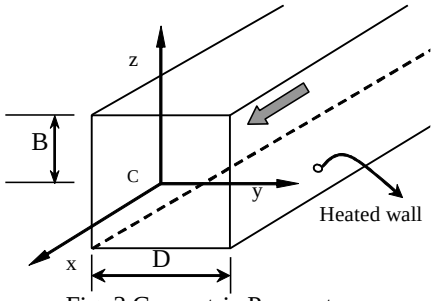

Fig: 3 Geometric Parameters and Wall Coordinate System

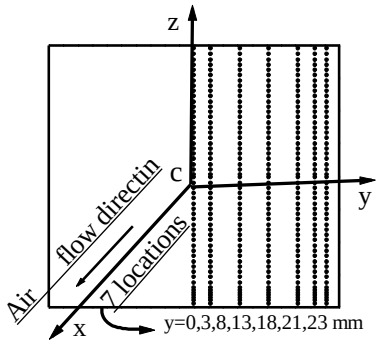

Fig:4 Dots represents 105 probe positions in space at each location

The geometric parameters, coordinate system, and the flow direction are schematically shown in Fig: 3. The time mean velocity and the static pressure are measured by the United Sensor (USA) pitot static tube of 1.6 mm outer diameter with a Furnace Controls Ltd. (U.K), pressure transducer (model MDC FC001 and FC012 and a Keithly (USA) digital micro-voltmeter with a data logger system (model 2426). The signals of the pitot static tube are transmitted to pressure transducer through 1.4 mm bore flexible tygon tubing. The signals of the digital micro-voltmeter correspond to the velocity head of the pitot static tube.

Before starting the experiment, the output voltage for the pressure transducer for different range of scale is calibrated in the calibration rig with a Dwyer (USA) slack vertical water tube manometer for the velocity and with an Ellison (USA) inclined manometer, using Kerosene of specific gravity 0.7934, for static pressure measurement. For the measurement of all signals with micro-voltmeter, integration times of about 30 seconds are used. The bottom wall temperatures are measured by 24 copper constant thermocouples distributed along the entire length of the heated portion. The air temperature entering and leaving the heated portion are also measured by two thermocouples.

5. Data Reduction

The mean values of time mean velocity and temperature are calculated by integration of the local time mean velocity and temperature profile curve divided by the total length of the curve along the abscissa [5]. The net heat transfer rate can be calculated from,

$$q = \frac{Q}{A_c} = C_P G(\Delta T_{\ln}), \qquad where \quad \Delta T_{\ln} = \frac{(T_{bo} - T_{bi})}{\ln\left[\frac{(T_{wc} - T_{bi})}{(T_{wc} - T_{bo})}\right]} \tag{1}$$

The local outer wall temperature T_w is read from the thermocouple output. The corrected local inner wall temperature, T_{wc} for Eqn. (1) is calculated by one dimensional heat conduction equation [5] as:

$$T_{wc} = T_w - \left(\frac{Q\delta}{kA_c}\right) \tag{2}$$

The average value of local heat transfer coefficient h is evaluated from,

$$h = \frac{q}{(T_{wc} - T_b)} \tag{3}$$

The coordinate y indicating the location of probe position for measurement are non-dimensionalized by the half width of the duct, B=D/2 as y/B. The flow velocity recorded by data logger in millivolts is converted to velocity in (m/s) and pressure drop in (N/m^2) by calibration equations. Thermal conductivity depends on temperature. Since the air velocity and temperature varies along the duct, all the air properties and related parameters are calculated at the bulk mean air temperature and the bulk mean air velocity as given bellow [6]:

$$T_b = \frac{1}{2}(T_o + T_i) \quad \text{and} \quad u_b = \frac{1}{2}(u_o + u_i) \tag{4}$$

The local Nusselt's number, friction factor, and Stanton umber are calculated from the following relations as:

$$Nu_s = \frac{hD}{K_f} \tag{5}$$

$$f_s = \left(\frac{\Delta p}{\Delta L}\right) \cdot \frac{D}{\left[\rho \bar{u}^2 / 2\right]} \tag{6}$$

$$St_s = \frac{h}{[\rho c_p u_b]} \tag{7}$$

6. Data Analysis

Since the duct is heated asymmetrically at the bottom wall only, it is symmetric about z-axis but asymmetric about the y-axis Fig.:3. The measurements are taken only in one half of the cross section about the symmetrical axis as shown in Fig.:4, which represent the flow characteristics of the entire duct. Measurements are made at the section x=34.5D downstream from the leading edge of the heated section i.e. x=94.56D from the unheated section. In this position both velocity and temperature fields can be considered to be fully developed. The time mean velocity and temperatures of air are measured within the region of -25mm<z<25 mm (i.e. -1<z/B<1) and 0≤y≤23 mm (i.e.0≤y/B≤0.92) at 7 different locations of y = 0, 3, 8, 13, 18, 21, and 23 mm (i.e., y/B=0.0, 0.12, 0.32, 0.52, 0.72, 0.84, and 0.92) in the cross section. The time mean velocity and the temperature are calculated from the probability distribution function of the measurements recorded by the data logger. There are typically 105 measurement points in space at each measuring location and a total of 105×7=735 points in space for half of the cross section of the duct which represents the data for the entire duct cross section. The measurements are taken for 10 different Reynolds Number varying between 5×10^4< Re< 1×10^5.

The corresponding statistical error is between 0.55 to 1.85 percent in the time mean velocity and between 1.23 to 2.06 percent in the temperature. The scattering of the wall temperature measurement is found to be between 2.0 to 3.5 percent and the uniformity of the wall temperature distribution is considered to be satisfactory, [9]. The time mean velocity measurements are repeated whenever error or doubtful situations occurred to ensure that the measured results are repeatable.

7. Results and Discussions

The longitudinally constant heat flux boundary condition of the present investigation, thermally fully developed region is characterized by wall and air temperature that increases linearly as a function of longitudinal positions, [2] and [6]. The experimental results concerning Nusselt's number, friction factor and Stanton number obtained for a turbulent flow through an asymmetrically heated smooth square duct with constant heat flux as the boundary condition are discussed briefly.

Nusselt's Number

Fig: 5 show the effect of Reynolds Number on local Nusselt's number at constant pressure drop. At constant pressure drop local Nusselt's number decrease rapidly with negligible decrease of the local Reynolds Number in the region y/B <0.52, but above the region y/B>0.52 towards the side walls the local Nusselt's number increases linearly with the decrease of Reynolds Number. This reflects the effect of the secondary flow in the region 0.72> y/B> 0.32 i. e. the secondary flow carrying primary velocity with higher temperature from the centre of the duct towards the corner along the corner bisector of the duct the mixing up of cold air with hot air and increases the turbulent intensity which intern causes the corresponding air temperature to rise thus increasing the heat transfer there and hence the Nusselt's number increases from the centre towards the side walls. With the increase of static pressure drop the curves shift up towards right. These characteristics are clearly seen in Fig; 6 showing the distributions of local Nusselt's number at constant Reynolds Number across the duct. The local Nusselt's number increases linearly with increase of y/B from centre towards the side walls at constant Reynolds Number. The nature of variation of Nusselt's number with increase of positions y/B, Fig: 6, is similar to that of local variation of heat transfer coefficient. With the increase of Reynolds Number the Nesselts number curve shifts up in a similar manner as that of heat transfer [1]. In the present experimental investigation it is found that on average, with 57.44 percent increase in Reynolds Number the static pressure drop is increased by 185.61 percent and the Nusselt's number is increased by 40.63 percent. Finally the local data in the fully developed region are compared and correlated with Prandl number as variable parameter is shown in Fig: 7. It can be seen that the Nusselt'ss number increases linearly with the increase of Reynolds Number at each location of measurement y/B. Fig: 7 also shows that the curve shifts up with increase of y/B from the centre of the duct towards the side walls. In the present investigation it found that the results obtained compared well the published data. The correlations developed are expressed as follows:

$$\overline{Nu}_{S,V} = 177.47 + 14.89\left(\frac{y}{B}\right) \quad \text{(Fig. 6)} \tag{8}$$

$$\overline{Nu}_S = 0.046\,\mathrm{Re}^{0.753}\,\mathrm{Pr}^{0.4} \quad \text{(Fig. 7)} \tag{9}$$

Symbols for Fig: 5

□ Δp_1=1.08, ○ Δp_2=1.26, △ Δp_3=1.47, ▽ Δp_4=1.67, ◇ Δp_5=1.85, + Δp_6=2.09, × Δp_7=2.46, ✳ Δp_8=2.67, – Δp_9=2.88, | Δp_{10}=3.07.

Symbols for fig: 6

□ Re=55874, ○ Re=60666, △ Re=64029, ▽ Re=67490, ◇ Re=70500, + Re=74043, × Re=79923, ✳ Re=82712, – Re=85366, | Re=87970.

Symbols for Fig: 7 □ y/B=0, ○ y/B=0.12, △ y/B=0.32, ▽ y/B=0.52, ◇ y/B=0.72, + y/B=0.84, × y/B=0.92.

– – Nu_s, Fujita, 1989;

· · · Nu_s, Mc Adams

– · – Nu_s, Modified Dittus-Boelter;

– · · – Nu_s, flat plate.

Solid lines represent present correlations.

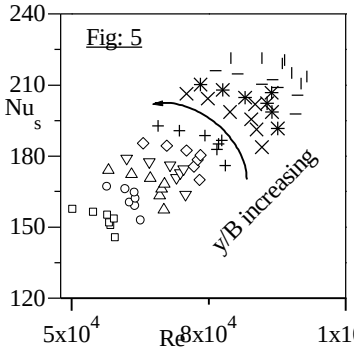

Fig: 5 Effect of Reynolds Number on local Nusselt's number.

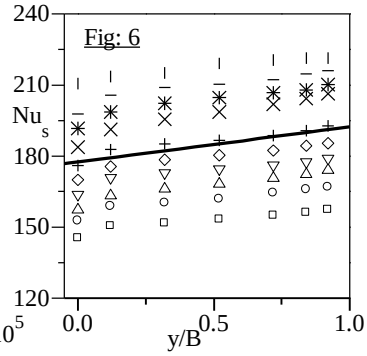

Fig: 6 Distributions of local Nusselt's number.

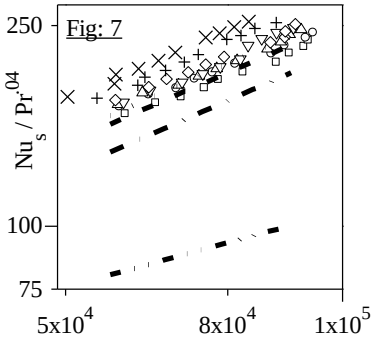

Fig: 7 Comparison of local friction factors.

Symbols for Fig: 8 □ Δp_1=83.81, ○ Δp_2=98.05, △ Δp_3=114.61, ▽ Δp_4=129.74, ◇ Δp_5=144.00, + Δp_6=162.68, × Δp_7=191.45, ✳ Δp_8=207.87, – Δp_9=224.07, | Δp_{10}=239.35.

Symbols for fig: 6 □ Re=55874, ○ Re=60666, △ Re=64029, ▽ Re=67490, ◇ Re=70500, + Re=74043, × Re=79923, ✳ Re=82712, – Re=85366, | Re=87970.

Symbols for Fig: 10 □ y/B=0, ○ y/B=0.12, △ y/B=0.32, ▽ y/B=0.52, ◇ y/B=0.72, + y/B=0.84, × y/B=0.92.

– – f_s Blasius (Liou et al., 1992);

· · · f_s Rohsenow & Choi, 1969.

Δp is in N/m^2.

Solid lines represent Present correlations:

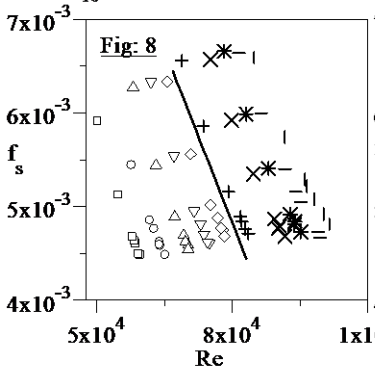

Fig: 8 Effects of Reynolds Number on local friction factors.

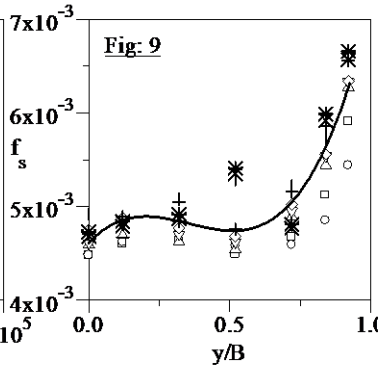

Fig: 9 Distributions of local friction factors.

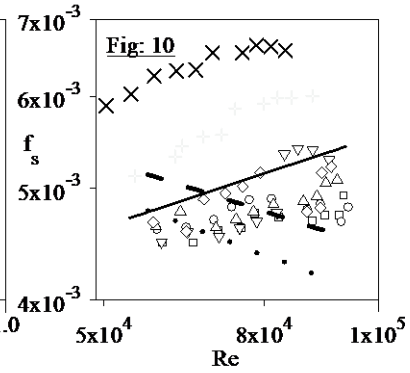

Fig: 10 Comparison of local friction factors.

These equations (7) and (8) are valid for 80< Δp< 240 N/m^2 and 5×10^4< Re< 1×10^5 at constant heat flux boundary condition.

The local as well as the average values of Nusselt's number are compared with some of the well-known published data. The secondary flow pattern in the duct is reflected in the local distributions of the Nusselt's number the values of which on the asymmetrically heated bottom wall of the smooth square duct are 1.04 to 1.22 times higher compared with the well-known published data for smooth circular ducts. Since it is found that, for the same experimental set up, the top half of the duct behaves like a flat plat [3], the results are compared with the published data for the flat plate as shown in Fig: 7, the Nusselt's number obtained in the present investigation is 2.32 times higher compared with that of the flat plate.

Friction Factor and Stanton number

The effects of Reynolds Number on both the local friction factor and the local Stanton number for fully developed flows with constant heat flux are depicted in Fig: 8 and 11 respectively. The characteristics of both curves are similar. Both the local friction factor and the local Stanton number increase linearly at constant

pressure drop with the decrease of Reynolds Number from center towards the side walls. Fig: 8 and 11 also show that with the increase of the pressure drop both the local friction factor and Stanton number curves shifts up towards the right but the corresponding values of friction factor and Stanton number gradually increasing and decreasing respectively with increase of pressure drop Δp. This trend is clearly visible in Fig: 9 and 12, where both the friction factor and Stanton number increase with the increase of y/B at constant Reynolds Number. In Fig: 9 and 12, the distributions of both the friction factor and the Stanton number across the duct at different Reynolds Number are displayed. It is found that with 58 percent increase in Reynolds Number the friction factor and Stanton number increase by 36 percent and 25 percent respectively. These variations of the local friction factor and the Stanton number can be expressed by third degree polynomial equations as follows:

$$\bar{f}_S = 0.0046 + 0.0022\left(\frac{y}{B}\right) - 0.0089\left(\frac{y}{B}\right)^2 + 0.0092\left(\frac{y}{B}\right)^3 \qquad \text{(Fig. 8) (10)}$$

$$\bar{St}_S = 0.0032 + 0.0015\left(\frac{y}{B}\right) - 0.0042\left(\frac{y}{B}\right)^2 + 0.0039\left(\frac{y}{B}\right)^3 \qquad \text{(Fig. 11) (11)}$$

These equations (10) and (11) are valid for $80 < \Delta p < 240\ N/m^2$ and $5\times10^4 < \mathrm{Re} < 1\times10^5$ at constant heat flux boundary condition.

For the same experimental set up and boundary condition the results obtained for both Nusselt's number and Stanton number shown in Fig: 7 and Fig: 13 respectively agree well with published data but the results obtained for the friction factor does not agree as shown in Fig: 10. With the increase of Reynolds Number the viscosity of air increases, the increased heat transfer in the asymmetrically heated duct is achieved at the expense of increased friction due to increase of both primary as well as secondary flow of air flow. Since the viscosity is

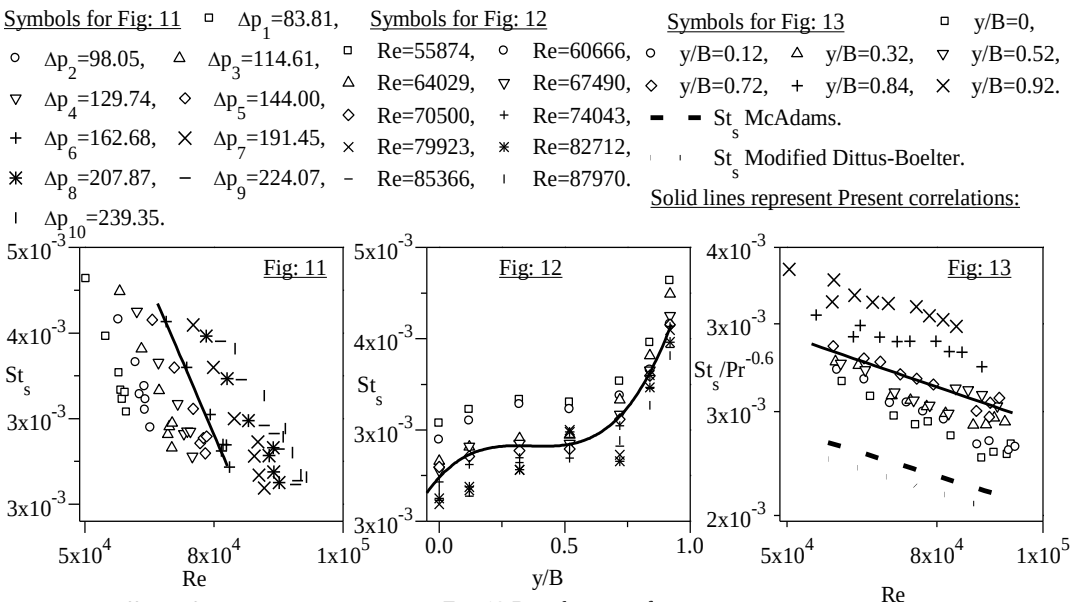

Fig: 11 Effects of Reynolds Number on local Stanton number.

Fig: 12 Distributions of local Stanton number.

Fig: 13 Comparions of Stanton numbers.

increasing with the increase of Reynolds Number the friction factor must also increase. Also it can be seen in the Darcy's formula, $f = \dfrac{(\Delta p/\Delta L)/D}{\frac{1}{2}\rho v^2}$, $f \propto \dfrac{\Delta p}{u^2}$, assuming all other parameters are constant, the ratio of $\dfrac{\Delta p}{u^2}$ increases with the increase of pressure drop. Hence the friction factor increases with the increases of Reynolds Number instead of decreasing as that of the published data. The improved correlations obtained are as follows:

$$\bar{f}_S = 0.003\,\mathrm{Re}^{0.261} \qquad \text{(Fig. 10) (12)}$$

$$\bar{St}_S = 0.0034\,\mathrm{Re}^{-0.221}\,\mathrm{Pr}^{-0.6} \qquad \text{(Fig. 13) (13)}$$

These equations (12) and (13) are valid for $5\times10^4 < \mathrm{Re} < 1\times10^5$ at constant heat flux boundary condition.

In the present investigation the friction factor obtained increases with the increase of Reynolds Number instead of published data where it decreases or approaches a constant value for smooth noncircular ducts. Comparing with the published data the friction factor and the Stanton number the results obtained in the present investigations are respectively 1.07 to 1.17 and 1.17 to 1.20 times higher than those of smooth circular duct. The results are presented in their final concise form of compact correlations that involve dimensionless groups which

represent the characteristics of the friction factor and the Stanton number. These correlations can be used for improved numerical analysis and for better design of heat transfer equipment for engineering applications.

8. Acknowledgments

This is a part of PhD woks carried out at BUET, Dhaka, by the first author under the guidance of the second and third authors. The first author is grateful to BUET authorities and staffs, the panel of expert referees, especially the second author for their comments and suggestions, which led to substantial improvement of this work. The first author is also grateful to the forth author for editing and formatting the paper including figures, tables etc.

9. References

[1] A.K.M.A. Hamid, A.R. Akanda, and M.A.T. ALI, "The Time Velocity and Temperature Fields in Developed Region in an Asymmetrically Heated Smooth Square Duct." *Journal of Engineering and Technology*, ISSN 1684-4114, Vol. 9 No. 2, December 2011.

[2] A.K.M.A. Hamid, "Experimental Study on Convective Heat Transfer with Turbulence Promoters", *Ph.D. thesis*, Bangladesh University of Engineering and Technology, Dhaka, Bangladesh, 2004.

[3] F.B. Gessner,"Turbulence and Mean-flow Characteristics of Fully Developed flow in Rectangular Channels," *Ph.D. Thesis*, Dept. Mech. Engg. Purdue University, 1964.

[4] F.B. Gessner, and A.F. Emery, "A Length-Scale Model for Developing Turbulent Flow in a Rectangular Duct," *ASME Journal of Fluids Engineering*, Vol. 103, pp. 445-455, 1981.

[5] J.C. Han, "Heat Transfer and Friction in Channels with Two Opposite Rib-Roughened Walls," *ASME Journal of Heat Transfer*, Vol. 106, No. 4, pp. 774-781, 1984.

[6] M. Hirota, H. Fujita, and Yokosawa, "Experimental study on convective heat transfer for turbulent flow in a square duct with a ribbed rough wall (characteristics of mean temperature field)," *ASME Journal of Heat Transfer*, Vol. 116, pp.332-340, 1994.

[7] W.M. Kays, and M.E. Crawford, "Convective Heat and Mass Transfer", *McGraw-Hill*, New York, 1980.

[8] S.J. Kiline, and F. A. McClintock, "Describing Uncertainties in Single-Sample Experiments," *Mechanical Engineering*, Vol. 75, pp. 3-8, 1953.

[9] K. Komori, A. Iguch, and R. Iguni, "Characteristics of fully developed Turbulent flow and Mass Transfer in a Square Duct." *International Chemical Engineering*, 20. (2), pp. 219-225, 1980.

10. Nomenclature

A = Area	m^2
B = Half of width of duct	M
C = Specific heat, Centre	$W.s/kg^OC$
D = Hydraulic diameter of duct	M
f = Friction factor	Dimensionless
G = Mass flux	Kg/m^2s
h = Heat transfer coefficient	$W/(m^2, {}^0C)$
k = Thermal conductivity	$W/(m, {}^0C)$
L = Length	M
Nu = Nusselt number	Dimensionless
P = Pressure	N/m^2
Pr = Prandtl number	Dimensionless
q = Heat flux	W/m^2
Q = Heat transfer	W
Re = Reynolds' number	Dimensionless
Re = Reynolds' number	Dimensionless
T = Mean temperature	^0C
x,y,z = Coordinate system	

10.1 Greek letters

τ = Shear stress	N/m^2
ν = Kinematics iscosity	m^2/s
ρ = Density	kg/m^3
δ = Aluminum wall thickness	Mm

10.2 Subscripts

a = Ambient temperature	f = Fluid
b = Bulk mean	i = Inlet
C = Centre, correct	in = Input
L = Loss	m = Mean
o = Outlet	w = Wall
s = Smooth duct, surface	ln = Log mean